

Research Article

Sensitivity of Multicarrier Two-Dimensional Spreading Schemes to Synchronization Errors

Youssef Nasser,¹ Mathieu des Noes,¹ Laurent Ros,² and Geneviève Jourdain²

¹CEA-LETI, 17 rue des Martyrs, 38054 Grenoble Cedex 09, France

²GIPSA-Lab/ DIS, INPG, BP 46, 38402 Saint Martin d'Hères, France

Correspondence should be addressed to Youssef Nasser, youssef.nasser@ieee.org

Received 12 July 2007; Revised 9 January 2008; Accepted 6 April 2008

Recommended by Soura Dasgupta

This paper presents the impact of synchronization errors on the performance of a downlink multicarrier two-dimensional spreading OFDM-CDMA system. This impact is measured by the degradation of the signal to interference and noise ratio (SINR) obtained after despreading and equalization. The contribution of this paper is twofold. First, we use some properties of random matrix and free probability theories to derive a new expression of the SINR. This expression is then independent of the actual value of the spreading codes while still accounting for the orthogonality between codes. This model is validated by means of Monte Carlo simulations. Secondly, the model is exploited to derive the SINR degradation of OFDM-CDMA systems due to synchronization errors which include a timing error, a carrier frequency offset, and a sampling frequency offset. It is also exploited to compare the sensitivities of MC-CDMA and MC-DS-CDMA systems to these errors in a frequency selective channel. This work is carried out for zero-forcing and minimum mean square error equalizers.

Copyright © 2008 Youssef Nasser et al. This is an open access article distributed under the Creative Commons Attribution License, which permits unrestricted use, distribution, and reproduction in any medium, provided the original work is properly cited.

1. INTRODUCTION

Recently, orthogonal frequency and code division multiple access technology have been investigated for the next generation of mobile communication systems [1, 2]. It is a combination of orthogonal frequency division multiplexing (OFDM) and code division multiple access (CDMA).

To achieve high spectrum efficiency, these systems will implement a large number of subcarriers, and, as a consequence, will be highly sensitive to synchronization errors. More specifically, when the transmitter and receiver are not synchronized, intercarrier interference (ICI) and possibly intersymbol interference (ISI) are generated at the receiver, which degrade the signal to interference and noise ratio (SINR). This effect has been intensively studied for OFDM systems [3–5]. Concerning multicarrier CDMA (MC-CDMA) and multicarrier direct sequence CDMA (MC-DS-CDMA) schemes, their sensitivities to sampling and carrier errors have been evaluated in [6–8]. To derive an analytic expression of the SINR, these articles considered the particular case of a Gaussian channel and a zero forcing (ZF) equalizer. Moreover, they assume that the chips of the spreading sequences are independent and identically dis-

tributed (i.i.d.) binary random variables. This is the classical random spreading assumption. Unfortunately, this model is not accurate for the downlink of CDMA or OFDM-CDMA systems, since it does not take into account the orthogonality between codes when using isometric sequences matrices like Walsh-Hadamard (WH) type. When using an isometric spreading matrix, the codes are no longer independent.

The contribution of this article is twofold. First, a generalized framework is proposed for modelling the effect of synchronisation errors on two-dimensional spreading called thereafter OFDM-CDMA systems. This encompasses the particular cases of MC-CDMA and MC-DS-CDMA. Then, exploiting some results from the random matrix (RM) and free probability (FP) theories, an analytic expression of the SINR modeling the impact of a synchronization error is derived. This model works for frequency selective channels and any single user detector. The sophisticated detectors such as the multiuser detector [9] or the iterative detectors [10] are out of scope of the paper. However, we give a brief overview about these detectors in Appendices. To derive the SINR formula, the mathematical background developed in [11, 12] and our works in [13, 14] have been reused. The SINR formula is independent from the actual

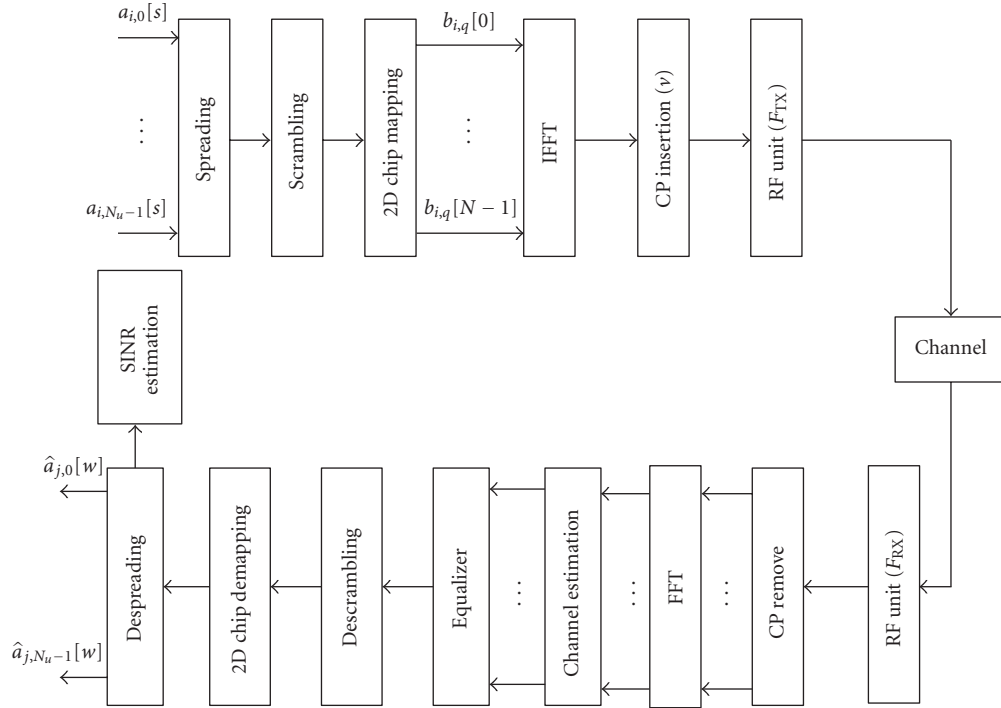


FIGURE 1: OFDM-CDMA transceiver.

values of the spreading codes while taking into account their orthogonality. This is the main novelty of this article. To confirm the validity of the proposed model, the mean theoretical SINR is compared to the mean SINR measured via Monte Carlo simulation. The model is then exploited to compare the sensitivities of MC-CDMA and MC-DS-CDMA systems to different synchronization errors in a frequency selective channel with ZF or minimum mean square error (MMSE) equalizers.

This article is structured as follows. Section 2 describes the transmission model for OFDM-CDMA systems with synchronization errors. Section 3 derives an asymptotic expression of the SINR using some properties of the RM theory. Section 4, first, validates the proposed model by means of simulations, and then the SINR formula is exploited to compare the sensitivities of different spreading schemes to synchronization errors. Eventually, conclusions are drawn in Section 5.

In order to simplify the reading, the following notations are considered: the bold lower-face letters represent a vector notation, and bold capital letters represent the matrix notation. The variables u , k , and l represent the time domain. The variables s and n represent the frequency domain. The superscript $(\cdot)'$ indicates a parameter of interest at the receiver side.

2. SYSTEM MODEL

2.1. System description

In this section, the generalized framework describing an OFDM-CDMA system is presented. Figure 1 shows a

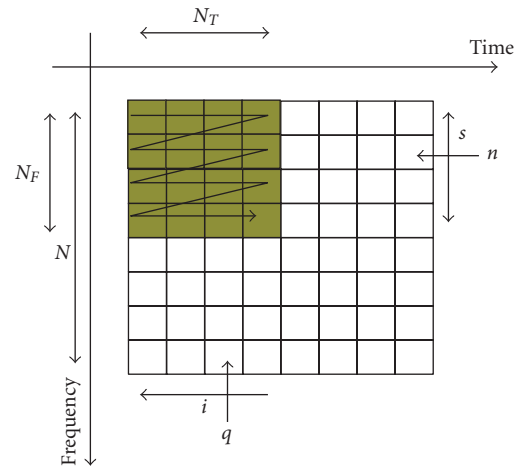


FIGURE 2: Time frequency grid.

two-dimensional (2D) spreading OFDM-CDMA transmitter/receiver (TX/RX) chain for a downlink communication with N_u users [1]. For each user, each symbol is first spread by a WH sequence of N_c chips and scrambled by a portion of N_c chips of the cell specific long pseudo random sequence. This scrambling code is used to minimize the multicell interference. The resulting chips are then allocated on the time-frequency grid as shown in Figure 2.

The first N_T chips are allocated in the time direction. The next blocks of N_T chips are allocated identically on adjacent subcarriers. The spreading factor is thus $N_c = N_F \cdot N_T$, where

N_F and N_T are, respectively, the frequency and time domain spreading factors. Each bin with coordinate (n, q) represents the signal transmitted on the n th subcarrier of the q th OFDM symbol. Other data symbols of the same user are spread in the same way in the next subbands. The scheme is identical for other users using one specific WH sequence by user, with $N_u \leq N_c$. The allocated chips are then transposed column wise to time domain using an inverse fast fourier transform (IFFT). Assuming an IFFT of N points, each user transmits $S = N/N_F$ data symbols $a_{i,m}[s]$ of the m th user on the i th OFDM-CDMA block. Particularly, for $N_T = 1$, the system resumes to a MC-CDMA [15], and for $N_F = 1$, it resumes to MC-DS-CDMA [16]. In the following, an OFDM symbol refers to the transmission of one IFFT at one time step $iN_T + q$, whereas an OFDM-CDMA block refers to the consecutive transmission of N_T OFDM symbols at the time step iN_T .

Given the above notations, the signal at the IFFT input is

$$b_{i,q}[sN_F + n] = \sum_{m=0}^{N_u-1} \sqrt{P_m} a_{i,m}[s] c_{m,s}[nN_T + q]$$

$$q = 0, \dots, N_T - 1; \quad s = 0, \dots, S - 1; \quad n = 0, \dots, N_F - 1, \quad (1)$$

where s is the index referring to the subband used for the transmission of the symbol $a_{i,m}[s]$ of the m th user. P_m is its transmit power which is identical in all subbands, $c_{m,s}$ represents its spreading sequence (chip by chip multiplication of the user assigned WH sequence and the cell specific scrambling code).

At the output of the IFFT, a cyclic prefix (CP) of v samples is inserted. The signal can be written as

$$x_{i,q}[k] = \sum_{s=0}^{S-1} \sum_{n=0}^{N_F-1} b_{i,q}[sN_F + n] \exp\left(j2\pi \frac{k(sN_F + n)}{N}\right),$$

$$k = -v, \dots, N - 1. \quad (2)$$

The sequence of samples is then fed at a rate $F_s = 1/T_s$ to a digital to analog converter (DAC), transposed to the TX carrier frequency F_{TX} by the radio frequency (RF) unit, and transmitted through the channel.

The signal at the RX side (Figure 1) is transposed to the base band with the RX carrier frequency F_{RX} and sampled at the receiver rate $F_r = 1/T_r$. The authors of [6] have introduced a general transmission model which includes the carrier frequency offset (CFO) and the sampling frequency offset (SFO) in the channel coefficient for a MC-CDMA system with a particular spreading assumption ($N = N_c$). The authors of [6] show that the received signal at the input of this particular case of MC-CDMA system could be written as

$$r_{q'}[u] = \sum_{n=0}^{N-1} b_{q'}[n] h_{q',q}^{\text{eq}}[n; u] \exp\left(j2\pi \frac{nu}{N}\right) + n_{q'}[u], \quad (3)$$

$$u = 0, \dots, N - 1,$$

where $h_{q',q}^{\text{eq}}[n; u]$ is an equivalent channel transfer function in frequency domain but changes at each sample u . It

TABLE 1: Simulation parameters.

FFT size (N)	64 subcarriers
Spreading length (N_c)	32 chips
System load	$\alpha = 1/4$ and $\alpha = 1$
Constellation	QPSK
Subcarrier spacing	312.5 KHz
Scrambling code	Concatenation of 19 gold codes of 128 chips
MC-CDMA	$N_F = 32, N_T = 1$
OFDM-CDMA	$N_F = 8, N_T = 4$
MC-DS-CDMA	$N_F = 1, N_T = 32$

includes only the time variation of the channel, the CFO, and the SFO. In our work, we will adapt their model to an OFDM-CDMA system by including all possible synchronization errors, that is, timing error, CFO, SFO, phase noise, and so forth. Nevertheless, the adaptation is quite difficult. Then, we give the details in Appendix A.

Based on this adaptation, the base-band time-discrete received signal can be written, after guard time removal, with the IFFT of the product of the data bins in the frequency domain by the channel transfer function coefficients (see Appendix A (A.7)):

$$r_{i',q'}[u] = \sum_{i=i'-1}^{i'+1} \sum_{s=0}^{S-1} \sum_{n=0}^{N_F-1} \sum_{q=0}^{N_T-1} \left[b_{i,q}[sN_F + n] \cdot h_{i',N_T+q',iN_T+q}^{\text{eq}}[sN_F + n; u] \exp\left(j2\pi \frac{(sN_F + n)u}{N}\right) \right]$$

$$+ n_{i',q'}[u], \quad u = 0, \dots, N - 1, \quad (4)$$

where the subscripts i', q' represent, respectively, the OFDM-CDMA block and the OFDM symbol of interest at the receiver. $n_{i',q'}[u]$ represents the zero mean additive white Gaussian noise (AWGN) with variance σ^2 .

Equation (4) appears difficult to interpret. Therefore, a better understanding of this equation is clearly needed in simple cases. That is, the expression $h_{i',N_T+q',iN_T+q}^{\text{eq}}[sN_F + n; u]$ evaluates the equivalent channel on the subcarrier n of the subband s taking into account the three possible synchronization errors: the timing error k_0 , the residual CFO $\Delta F = F_{RX} - F_{TX}$, and the residual SFO $1/\Delta T = 1/(T_r - T_s)$. It evaluates the equivalent channel applied on the $(iN_T + q)$ th transmitted OFDM symbol, where its effect is measured on the $(i'N_T + q')$ th received OFDM symbol. Eventually, the sums over i and q represent the ISI due to the timing error of k_0 samples with respect to the perfect position of the fast fourier transform (FFT) window at the receiving side. Moreover, for a perfect synchronized system, $h_{i',N_T+q',iN_T+q}^{\text{eq}}[sN_F + n; u]$ becomes independent of the time variable u . In this case, it represents $h_{i,q}[sN_F + n]$ the FFT on the subcarrier n of the subband s of the discrete low-pass

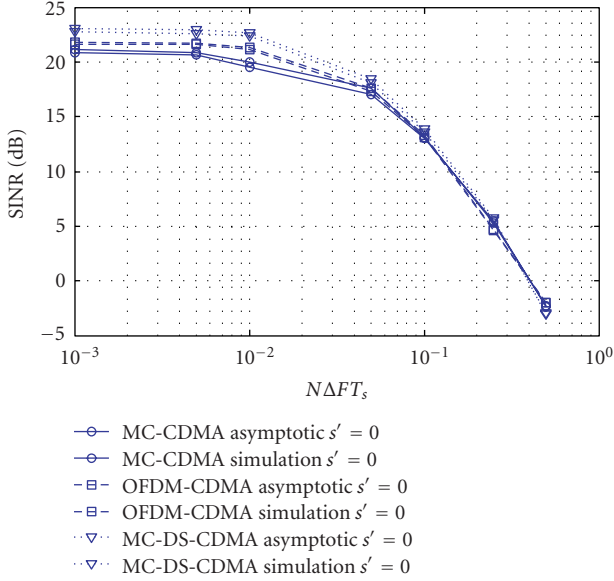


FIGURE 3: Validation of theoretical model (BRAN A).

physical channel $g_{iN_T+q}[k]$; $k = 0, \dots, W - 1$ with delay spread W samples ($W < \nu$). In this case, (4) yields

$$r_{i',q'}[u] = \sum_{s=0}^{S-1} \sum_{n=0}^{N_F-1} b_{i',q'}[sN_F+n] h_{i',q'}[sN_F+n] e^{j2\pi((sN_F+n)/N)u} + n_{i',q'}[u], \quad u = 0, \dots, N-1. \quad (5)$$

In this paper, we assume that the sampling and carrier errors linearly increase during one OFDM symbol only, that is, they are set to zero at the beginning of each OFDM symbol. Therefore, (4) yields for a carrier frequency error as

$$r_{i',q'}[u] = e^{j\theta_{i',q'}[u]} \sum_{s=0}^{S-1} \sum_{n=0}^{N_F-1} b_{i',q'}[sN_F+n] \times h_{i',q'}[sN_F+n] e^{j2\pi((sN_F+n)/N)u} + n_{i',q'}[u], \quad \text{with } \theta_{i',q'}[u] = 2\pi\Delta FT_s u, \quad u = 0, \dots, N-1. \quad (6)$$

For a sampling frequency offset, (4) yields

$$r_{i',q'}[u] = \sum_{s=0}^{S-1} \sum_{n=0}^{N_F-1} b_{i',q'}[sN_F+n] h_{i',q'}[sN_F+n] \cdot \left(e^{j2\pi((sN_F+n)/N)u} e^{j((sN_F+n)/N)\theta_{i',q'}[u]} + n_{i',q'}[u] \right) \quad \text{with } \theta_{i',q'}[u] = 2\pi \frac{\Delta T}{T_s} u, \quad u = 0, \dots, N-1. \quad (7)$$

Notice that, since we use a discrete representation of the transmission, the coefficients $g_{iN_T+q}[k]$ of the discrete channel can be expressed as a function of the parameters of the analog channel model by $g_{iN_T+q}[k] = \sum_{\ell=0}^{L-1} \alpha_{i,q}^{(\ell)}$.

$\text{sinc}\{\pi F_s(k/F_s - \tau_{i,q}^{(\ell)})\}$, where $\alpha_{i,q}^{(\ell)}$ and $\tau_{i,q}^{(\ell)}$ are, respectively, the complex amplitudes and the delays of the ℓ th multipath, and $\text{sinc}(x) = \sin(x)/x$.

The receiver selects N samples and transposes them to the frequency domain thanks to the FFT operation. At the output of the FFT module, the value of $s'(N_F + n')$ th subcarrier of the (q') th OFDM symbol of the (i') th OFDM-CDMA block is given by

$$R_{i',q'} = \sum_{i=i'-1}^{i'+1} \sum_{s=0}^{S-1} \sum_{n=0}^{N_F-1} \sum_{q=0}^{N_T-1} b_{i,q}[sN_F+n] \varphi_{i',i}(s',s,n',n,q',q) + N_{i',q'}[s'N_F+n'], \quad (8)$$

where s' is the desired subband index ($s' = 0, \dots, S-1$), and n' is the index of a subcarrier in the (s') th subband ($n' = 0, \dots, N_F-1$). $\varphi_{i',i}(s',s,n',n,q',q)$ is the “frequency side-to-side” (IFFT-channel-FFT) equivalent channel transfer function including the effect of the synchronization errors. It is given by

$$\varphi_{i',i}(s',s,n',n,q',q) = \frac{1}{N} \sum_{u=0}^{N-1} \exp\left(-j2\pi \frac{(s'-s)N_F + (n'-n)}{N} u\right) \cdot h_{i',i}^{\text{eq}}[s'N_F+n', iN_T+q][sN_F+n; u]. \quad (9)$$

We check that when there is no synchronization error, the function $\varphi_{i',i}(s',s,n',n,q',q)$ is equal to

$$\varphi_{i',i}(s',s,n',n,q',q) = \begin{cases} h_{i',q'}[s'N_F+n'] & \text{if } i' = i, s' = s, \\ & n' = n, q' = q, \\ 0 & \text{elsewhere.} \end{cases} \quad (10)$$

For a carrier frequency offset, the function φ is independent of the time indices i and q . Equation (9) is given by

$$\varphi_{i',i'}(s',s,n',n,q',q') = h_{i',q'}[sN_F+n] \Psi_N\left(\Delta FT_s + \frac{(s'-s)N_F + (n'-n)}{N}\right) \cdot \exp\left(j\pi(N-1)\left(\Delta FT_s + \frac{(s'-s)N_F + (n'-n)}{N}\right)\right), \quad (11)$$

where $\Psi_N(x)$ is the function defined by $\Psi_N(x) = \sin(\pi N x)/N \sin(\pi x)$. For $\Delta F = 0$, (11) yields

$$\varphi_{i',i'}(s',s,n',n,q',q') = \begin{cases} h_{i',q'}[s'N_F+n'] & \text{if } s' = s, n' = n, \\ 0 & \text{elsewhere.} \end{cases} \quad (12)$$

Once again, for a sampling frequency offset such that $\Delta T/T_s < 1/(N + \nu)$, (9) is independent of i and q . It is given by

$$\begin{aligned} & \varphi_{i',i'}(s', s, n', n, q', q') \\ &= h_{i',q'}[sN_F + n] \psi_N \left(\frac{sN_F + n}{N} \frac{\Delta T}{T_s} + \frac{(s' - s)N_F + (n' - n)}{N} \right) \\ & \cdot \exp \left(j\pi(N - 1) \left(\frac{sN_F + n}{N} \frac{\Delta T}{T_s} + \frac{(s' - s)N_F + (n' - n)}{N} \right) \right). \end{aligned} \quad (13)$$

Once again, we verify that (12) holds for a sampling offset $\Delta T = 0$.

For a timing synchronization error and due to ISI, (9) yields

$$\begin{aligned} & \varphi_{i',i}(s', s, n', n, q', q) \\ &= \frac{1}{N} \sum_{u=0}^{N-1} \exp \left(-j2\pi \frac{(s' - s)N_F + (n' - n)}{N} u \right) \\ & \cdot \exp \left(j2\pi(\beta + k_0) \frac{sN_F + n}{N} T_s \right) \\ & \sum_{l=M_1}^{M_2} g_{i,q}[l] \exp \left(-j2\pi \frac{sN_F + n}{N} l \right) \\ & \text{with } M_1 = [u - (N - 1)]T_s + \beta T_s + k_0 T_s, \\ & M_2 = (u + \nu)T_s + \beta T_s + k_0 T_s, \\ & \beta = (i' - i)N_T(N + \nu) + (q' - q)(N + \nu). \end{aligned} \quad (14)$$

The signal at the FFT output is multiplied the one-tap channel equalization coefficients $z_{i',q'}[s'N_F + n']$ and descrambled by the cell specific scrambling sequence used at the transmission. Then, it is multiplied by the spreading sequence of the decision device. The equalization coefficients correct simultaneously the effect of channel distortion and the synchronization error distortion.

Without loss of generality, we assume that one is interested by the symbols of user 0. In order to write the received signal with matrix-vector notation, the following matrices are defined:

- (i) $\mathbf{P} = \text{diag}(\sqrt{P_0}, \sqrt{P_1}, \dots, \sqrt{P_{N_u-1}})$ is the $N_u \cdot N_u$ diagonal matrix which entries are the signal amplitudes allocated to each user;
- (ii) $\mathbf{Q} = \text{diag}(\sqrt{P_1}, \sqrt{P_2}, \dots, \sqrt{P_{N_u-1}})$ is the $(N_u - 1) \cdot (N_u - 1)$;
- (iii) $\mathbf{C}[s] = (\mathbf{c}_0[s], \mathbf{c}_1[s], \dots, \mathbf{c}_{N_u-1}[s])$ is the $N_c \cdot N_u$ matrix containing all the spreading codes used in the s th subband;
- (iv) $\mathbf{U}[s] = (\mathbf{c}_1[s], \mathbf{c}_2[s], \dots, \mathbf{c}_{N_u-1}[s])$ is the $N_c \cdot (N_u - 1)$ matrix containing the codes of the interfering users in the s th subband. Both matrices $\mathbf{C}[s]$ and $\mathbf{U}[s]$ depend on subband index s because of the long scrambling code.

We also define the following vectors:

- (i) $\mathbf{a}_i[s] = (a_{i',0}[s], \dots, a_{i',N_u-1}[s])^T$ corresponds to the symbols of all users transmitted in the s th subband;
- (ii) $\tilde{\mathbf{a}}_i[s] = (a_{i',1}[s], \dots, a_{i',N_u-1}[s])^T$ corresponds to the symbols of interfering users transmitted in the s th subband.

The estimated symbol of the reference user on the subband (s') is then

$$\begin{aligned} \hat{a}_{i',0}[s'] &= I_0 a_{i',0}[s'] + I_1 + I_2 + I_3 + I_4, \\ I_0 &= \sqrt{P_0} \mathbf{c}_0^H[s'] \mathbf{Z}_{i'}[s'] \mathbf{H}_{i',i'}[s', s'] \mathbf{c}_0[s'], \\ I_1 &= \mathbf{c}_0^H[s'] \mathbf{Z}_{i'}[s'] \mathbf{H}_{i',i'}[s', s'] \mathbf{U}[s'] \mathbf{Q}[s] \tilde{\mathbf{a}}_i[s'], \\ I_2 &= \sum_{\substack{s=0 \\ s \neq s'}}^{s-1} \mathbf{c}_0^H[s'] \mathbf{Z}_{i'}[s'] \mathbf{H}_{i',i'}[s', s] \mathbf{C}[s] \mathbf{P}[s] \mathbf{a}_i[s], \\ I_3 &= \sum_{\substack{i=i'+1 \\ i \neq i'}}^{s-1} \sum_{s=0}^{s-1} \mathbf{c}_0^H[s'] \mathbf{Z}_{i'}[s'] \mathbf{H}_{i',i}[s', s] \mathbf{C}[s] \mathbf{P}[s] \mathbf{a}_i[s], \\ I_4 &= \mathbf{c}_0^H[s'] \mathbf{Z}_{i'}[s'] \mathbf{n}_{i'}[s']. \end{aligned} \quad (15)$$

Notation

\mathbf{A}^H is the transpose-conjugate of matrix \mathbf{A} .

In (15), I_0 represents the useful signal gain, I_1 the multiple access interference (MAI) generated in the same subband s' , I_2 the interference generated by all users from other subbands (inter band interference (IBI)), I_3 interference generated by code $\mathbf{c}_0[s']$ in blocks $i' - 1$ or $i' + 1$ (ISI depending on k_0), and I_4 the filtered noise. $\mathbf{H}_{i',i}[s', s]$ is an $N_c \cdot N_c$ matrix modeling the combined effect of the channel attenuation and the synchronization error. It is defined by

$$\begin{aligned} \mathbf{H}_{i',i}[s', s] &= \begin{pmatrix} \mathbf{A}_{i',i} R^* & \mathbf{A}_{i',i} R^{**} & \cdots & \mathbf{A}_{i',i} C \\ \mathbf{A}_{i',i} R' & \cdots & \cdots & \mathbf{A}_{i',i} C' \\ \vdots & \vdots & \vdots & \vdots \\ \mathbf{A}_{i',i} W' & \mathbf{A}_{i',i} W'' & \cdots & \mathbf{A}_{i',i} C' \end{pmatrix}, \\ \mathbf{A}_{i',i}[s', s, n', n] &= \begin{pmatrix} \varphi_{i',i} a' & \cdots & \varphi_{i',i} a^* \\ \varphi_{i',i} a'' & \ddots & \varphi_{i',i} a^{**} \\ \vdots & & \vdots \\ \varphi_{i',i} z^* & \cdots & \varphi_{i',i} z^{**} \end{pmatrix}, \end{aligned} \quad (16)$$

where R^* denotes $[s', s, 0, 0]$, R^{**} denotes $[s', s, 0, 1]$, C denotes $[s', s, 0, N_F - 1]$, R' denotes $[s', s, 1, 0]$, C' denotes $[s', s, 1, N_F - 1]$, W' denotes $[s', s, N_F - 1, 0]$, W'' denotes $[s', s, N_F - 1, 1]$, C' denotes $[s', s, N_F - 1, N_F - 1]$, a' denotes $(s', s, n', n, 0, 0)$, a^* denotes $(s', s, n', n, 0, N_T - 1)$, a'' denotes $(s', s, n', n, 1, 0)$, a^{**} denotes $(s', s, n', n, 1, N_T - 1)$, z^* denotes $(s', s, n', n, 0, N_T - 1, 0)$, and z^{**} denotes $(s', s, n', n, 0, N_T - 1, N_T - 1)$.

If there is no synchronization error, the matrix $\mathbf{H}_{i',i}[s',s]$ is the null matrix for $s' \neq s$ and it is a diagonal matrix when $i' = i$ and $s' = s$. In the latter case, I_2 and I_3 are equal to zero, that is, there is no IBI and no ISI.

$\mathbf{Z}_{i'}[s']$ is a $N_c \cdot N_c$ diagonal matrix which components are the equalizer's coefficients.

2.2. SINR evaluation

The symbols $a_{i,m}[s]$ are assumed i.i.d. random variables with zero mean and unit variance. The SINR for every subband s' for one channel realisation, noted instantaneous SINR, is deduced from (15) by calculating the variances over I_0 , I_1 , I_2 , I_3 and I_4 . However, knowing that the symbols transmitted over the different subbands are independent (and hence uncorrelated), this yields that the different interference components are uncorrelated. The SINR is thus obtained by

$$\text{SINR}[s'] = \frac{E|I_0|^2}{E|I_1|^2 + E|I_2|^2 + E|I_3|^2 + E|I_4|^2}. \quad (17)$$

The expectations in (17) over the data symbols and noise terms are given by

$$\begin{aligned} E|I_0|^2 &= P_0 \left| \mathbf{c}_0^H[s'] \mathbf{Z}_{i'}[s'] \mathbf{H}_{i',i}[s',s'] \mathbf{c}_0[s'] \right|^2, \\ E|I_1|^2 &= \mathbf{c}_0^H[s'] \mathbf{Z}_{i'}[s'] \mathbf{H}_{i',i}[s',s'] \mathbf{U}[s'] \mathbf{Q}^2 \mathbf{U}^H[s'] \\ &\quad \times \mathbf{H}_{i',i}^H[s',s'] \mathbf{Z}_{i'}^H[s'] \mathbf{c}_0[s'], \\ E|I_2|^2 &= \sum_{\substack{s=0 \\ s \neq s'}}^{S-1} \mathbf{c}_0^H[s'] \mathbf{Z}_{i'}[s'] \mathbf{H}_{i',i}[s',s] \mathbf{C}[s] \mathbf{P}^2 \mathbf{C}^H[s] \\ &\quad \times \mathbf{H}_{i',i}^H[s',s] \mathbf{Z}_{i'}^H[s'] \mathbf{c}_0[s'], \\ E|I_3|^2 &= \sum_{\substack{i=i'-1 \\ i \neq i'}}^{i'+1} \sum_{s=0}^{S-1} \mathbf{c}_0^H[s'] \mathbf{Z}_{i'}[s'] \mathbf{H}_{i',i}[s',s] \mathbf{C}[s] \mathbf{P}^2 \mathbf{C}^H[s] \\ &\quad \times \mathbf{H}_{i',i}^H[s',s] \mathbf{Z}_{i'}^H[s'] \mathbf{c}_0[s'], \\ E|I_4|^2 &= \frac{\sigma^2}{N_c} \text{tr}(\mathbf{Z}_{i'}[s'] \mathbf{Z}_{i'}^H[s']), \end{aligned} \quad (18)$$

where $\text{tr}(\mathbf{A})$ is the trace of matrix \mathbf{A} .

These expressions show that the SINR depends on the actual value of the spreading codes. Hence, (18) cannot be used practically due to its complexity and its sensitivity to the code allocation. Moreover, the receiver has to estimate it each time the set of used sequences is changed by the base transceiver station (BTS).

On the other hand, it is known in the literature that a SINR independent of the codes can be obtained by achieving an expectation over the spreading codes. This expectation assumes i.i.d. codes chips. However, when the spreading

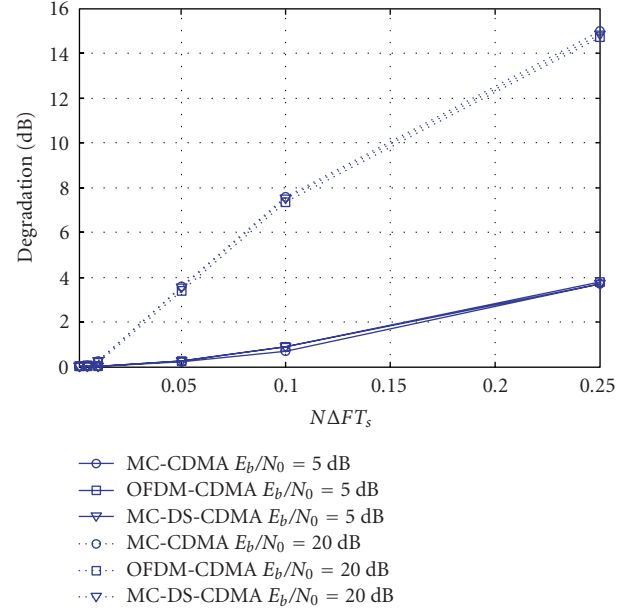


FIGURE 4: Comparison between degradation of different spreading schemes.

codes are isometric, this expectation does not achieve a SINR independent of the spreading codes since the orthogonality between them must be taken into account. In the sequel, we derive a new SINR formula that will be independent of the spreading codes while taking into account their orthogonality. This work relies on some results of RM and FP theories.

3. ASYMPTOTIC PERFORMANCE

The conceptual difficulty of the SINR estimation can be overcome by modeling the users' codes as random sequences. Tse and Hanly were the innovators of the application of RM theory to CDMA systems analysis [17]. They studied the asymptotic performance of the multiuser MMSE receiver for a CDMA system, assuming random spreading and synchronous reception. They found that the dependence of the SINR on the spreading codes was vanishing in the asymptotic regime ($N_c, N_u \rightarrow \infty$ while the ratio $\alpha = N_u/N_c$ is kept constant). The performances only depend on the system load α , the noise variance, and the power distribution. This work was then extended to a multipath fading channel in [18].

Unfortunately, the model with random sequence is not accurate for the downlink of CDMA or OFDM-CDMA systems, since it does not take into account the orthogonality between codes when using isometric sequences matrices like WH-type.

To solve this issue, the authors of [11] proposed a trick. They assume that the spreading matrix $\mathbf{C}[s]$ is extracted from a Haar distributed unitary matrix. Such a matrix is random and isometric, which captures the orthogonality of conventional spreading matrices. This assumption allows applying very powerful results from the FP theory. In [11, 12], it was

found that the aforementioned assumption is only technical. The simulation results obtained in [11, 12, 19] with the WH sequences match very well with the theoretical model. This is achieved even for relatively small spreading factors ($N_c \geq 32$).

In order to evaluate the different terms of (18) and get rid off the dependence on the spreading codes, we apply three properties from the RM and FP theories. The details of the computations are given in Appendix B. The final results are the following:

$$\begin{aligned}
 E|I_0|^2 &= P_0 \left| \frac{1}{N_c} \text{tr}(\mathbf{Z}_{i'}[s'] \mathbf{H}_{i',i'}[s',s']) \right|^2, \\
 E|I_1|^2 &= \alpha \bar{P} \left(\frac{1}{N_c} \text{tr}(\mathbf{Z}_{i'}[s'] \mathbf{H}_{i',i'}[s',s'] \mathbf{H}_{i',i'}^H[s',s'] \mathbf{Z}_{i'}^H[s']) \right. \\
 &\quad \left. - \left| \frac{1}{N_c} \text{tr}(\mathbf{Z}_{i'}[s'] \mathbf{H}_{i',i'}[s',s']) \right|^2 \right), \\
 E|I_2|^2 &= \frac{\alpha \bar{P}}{N_c} \sum_{\substack{s=0 \\ s \neq s'}}^{S-1} \text{tr}(\mathbf{Z}_{i'}[s'] \mathbf{H}_{i',i'}[s',s] \mathbf{H}_{i',i'}^H[s',s] \mathbf{Z}_{i'}^H[s']), \\
 E|I_3|^2 &= \frac{\alpha \bar{P}}{N_c} \sum_{i \neq i'}^{i'+1} \sum_{s=0}^{S-1} \text{tr}(\mathbf{Z}_{i'}[s'] \mathbf{H}_{i',i}[s',s] \mathbf{H}_{i',i}^H[s',s] \mathbf{Z}_{i'}^H[s']), \\
 E|I_4|^2 &= \frac{\sigma^2}{N_c} \text{tr}(\mathbf{Z}_{i'}[s'] \mathbf{Z}_{i'}^H[s']),
 \end{aligned} \tag{19}$$

where $\alpha = N_u/N_c$ is the system load and \bar{P} is the average power of the interfering users equal to $(1/(N_u - 1)) \sum_{m=1}^{N_u-1} P_m$.

The FP theory shows that $N_u \bar{P}$ is the power of total interfering users. However, since N_u and N_c must be as long as possible, $N_u \bar{P}$ can be assumed as the total transmitted power (including the power of the reference user).

We note that the FP theory is mainly used for the evaluation of $E|I_1|^2$, where the orthogonality between $\mathbf{c}_0^H[s']$ and $\mathbf{U}[s']$ must be taken into account. However, the RM theory is sufficient for the computation of the other terms in (19).

4. PERFORMANCE EVALUATION

Now, we will exploit (19) to compare the sensitivity of MC-CDMA, MC-DS-CDMA, and OFDM-CDMA spreading schemes to synchronization errors. In literature, we should note that some sophisticated equalizers could be used. These equalizers consider the MAI and ICI in the equalization process to the detriment of a complexity cost increase [9, 10]. They are rarely implemented in real systems. Even it is out of scope of the paper, we will give in Appendix C some results using an iterative receiver which copes with the introduced interference due to synchronization errors. In the sequel of the paper, we limit our study to a one-tap equalizer. First, we assume that the receiver uses a MMSE equalizer or a ZF equalizer. In an OFDM system, we can easily show that

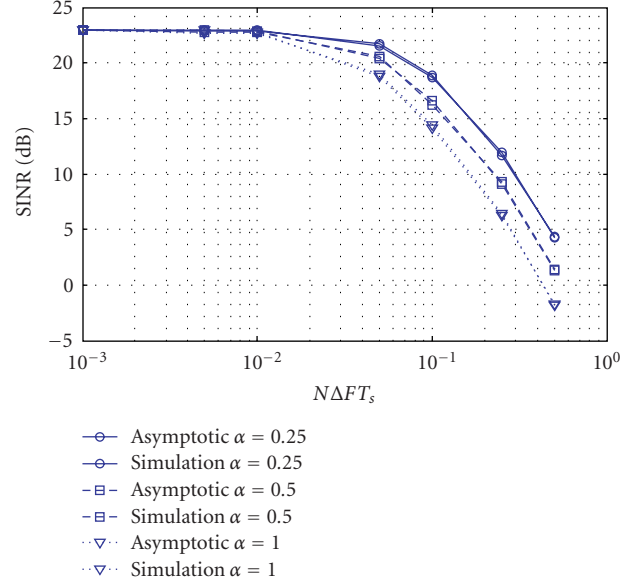


FIGURE 5: Sensitivity of MC-DS-CDMA to system load (Gaussian channel).

the MMSE and the ZF equalizers are equivalent, that is, they present the same performance. However, due to the spreading, it is not the case in OFDM-CDMA systems. The coefficients of the MMSE equalizer are given by

$$z_{i',q'}[s'N_F + n'] = \frac{\varphi_{i',i'}^*(s',s',n',n',q',q')}{|\varphi_{i',i'}(s',s',n',n',q',q')|^2 + \gamma}, \tag{20}$$

where γ is the normalized noise variance per subcarrier given by $\gamma = \sigma^2/\alpha \bar{P}$. The coefficients of the ZF equalizer are obtained by setting γ to zero.

Notice that according to (9), the coefficient $\varphi_{i',i'}(s',s',n',n',q',q')$ resumes to the time average during one OFDM symbol of the frequency equivalent channel, that is, $\varphi_{i',i'}(s',s',n',n',q',q') = (1/N) \sum_{u=0}^{N-1} h_{i',N_T+q',i',N_T+q'}^{\text{eq}}[s'N_F + n'; u]$. This implicitly assumes a perfect estimation of the “frequency side-to-side” equivalent channel transfer function $\varphi_{i',i'}(s',s',n',n',q',q')$ on the subcarrier $s'N_F + n'$.

In order to validate the asymptotic formula, we first compare the result computed with (19) with the instantaneous SINR measured via Monte Carlo simulations. Then, we define the instantaneous interference parameter $I[s'] = E|I_1|^2 + E|I_2|^2 + E|I_3|^2 + E|I_4|^2$ and the instantaneous degradation parameter $\text{Deg}_{(\text{dB})}[s'] = 10 \cdot \log_{10}(\text{SINR}_{\text{max}}[s']/\text{SINR}[s'])$, where $\text{SINR}_{\text{max}}[s']$ is the instantaneous SINR obtained for a perfectly synchronized system in the subband s' .

For a frequency selective slow fading physical channel and due to the variations of the channel caused by the mobile speed, we compare the average SINRs and we evaluate the average degradation and interference over channel realizations. The simulations performances are realized

for an average ratio \bar{E}_b/N_0 . It is given by $\bar{E}_b/N_0 = ((N + \gamma)/N) \cdot (\sum_{\ell=0}^{L-1} E(|\alpha_{i,q}^{(\ell)}|^2)/2\sigma^2) \cdot P_0$, where $E\{|\alpha_{i,q}^{(\ell)}|^2\}$ is the power of each multipath of the channel.

Since the different parameters depend on the type of synchronization error, three cases can be recognized in the sequel. The simulations assumptions are given in Table 1, unless they are notified.

4.1. Carrier frequency offset

For a carrier frequency offset, (19) yields

$$\begin{aligned}
 E|I_0|^2 &= P_0 \left| \frac{1}{N_F} \sum_{n'=0}^{N_F-1} \frac{|h_{i',q'}[Y'] \psi_N(X^*)|^2}{|h_{i',q'}[Y'] \psi_N(X^*)|^2 + \gamma} \right|^2, \\
 I[s'] &= \frac{\alpha \bar{P}}{N_F} \sum_{s=0}^{S-1} \sum_{n'=0}^{N_F-1} \sum_{n=0}^{N_F-1} \\
 &\quad \times \left| \frac{h_{i',q'}^*[Y'] h[Y''] \psi_N(X^*) \psi_N(X^* + X^{**})}{|h_{i',q'}[Y'] \psi_N(X^*)|^2 + \gamma} \right|^2 \\
 &\quad - \alpha \bar{P} \left| \frac{1}{N_F} \sum_{n'=0}^{N_F-1} \frac{|h_{i',q'}[Y'] \psi_N(X^*)|^2}{|h_{i',q'}[Y'] \psi_N(X^*)|^2 + \gamma} \right|^2 \\
 &\quad + \frac{\sigma^2}{N_F} \sum_{p=0}^{N_F-1} \left| \frac{h_{i',q'}[Y'] \psi_N(X^*)}{|h_{i',q'}[Y'] \psi_N(X^*)|^2 + \gamma} \right|^2, \\
 E|I_3|^2 &= 0,
 \end{aligned} \tag{21}$$

where Y' denotes $s'N_F + n'$, X^* denotes ΔFT_s , Y'' denotes $sN_F + n$, and X^{**} denotes $((s' - s)N_F + n' - n)/N$.

Figure 3 illustrates the comparison between theoretical and simulated average SINRs for the BRAN A channel model [20] and a mean ratio $\bar{E}_b/N_0 = 20$ dB. The SINRs have been measured in the first subband ($s' = 0$). Figure 3 shows that our theoretical model matches perfectly with simulations, even for a relatively small spreading factor ($N_c = 32$). As for conventional multicarrier systems, the degradation becomes noticeable for $N\Delta FT_s > 1\%$. Figure 4 gives the comparison between average degradation (over channel realizations) of different spreading schemes to carrier frequency offset for a full load and the Bran A channel model. It is suitable to conclude that the sensitivity of the 3 spreading schemes to carrier offset is comparable.

Figure 5 presents the sensitivity of the MC-DS-CDMA scheme to system load for a Gaussian channel. As predicted by (21), the degradation increases with the load. This result is in contradiction with the conclusion of [7] which stated that the MC-DS-CDMA scheme is not sensitive to system load since the MAI is eliminated by the equalizer for this spreading scheme.

Since the theoretical model has been validated, we will exploit (21) to give more insight on the sensitivities of MC-CDMA and MC-DS-CDMA to carrier frequency offset.

If the receiver implements a ZF equalizer ($\gamma = 0$), (21) yields

$$\begin{aligned}
 E|I_0|^2 &= P_0, \\
 I[s'] &= \frac{\alpha \bar{P}}{N_F} \sum_{s=0}^{S-1} \sum_{n'=0}^{N_F-1} \sum_{n=0}^{N_F-1} \left| \frac{h_{i',q'}[Y''] \psi_N(X^* + X^{**})}{h_{i',q'}[Y'] \psi_N(X^*)} \right|^2 \\
 &\quad - \alpha \bar{P} + \frac{\sigma^2}{N_F} \sum_{n'=0}^{N_F-1} \frac{1}{|h_{i',q'}[Y'] \psi_N(X^*)|^2},
 \end{aligned} \tag{22}$$

where Y'' denotes $sN_F + n$, X^* denotes ΔFT_s , X^{**} denotes $((s' - s)N_F + n' - n)/N$, and Y' denotes $s'N_F + n'$.

Let us note $I_{MC-DS-CDMA}[s']$, the interference power of the s' th subcarrier of a pure MC-CDMA scheme ($N_F = 1$, $N_T = N$, $S = N$), and $I_{MC-CDMA}$, the interference for a pure MC-CDMA system ($N_F = N$, $N_T = 1$, $S = 1$). Based on the above formula, we observe that

$$I_{MC-CDMA} = \frac{1}{N} \sum_{s'=0}^{N-1} I_{MC-DS-CDMA}[s']. \tag{23}$$

With a ZF equalizer, the total interference power of a MC-CDMA system is the average of the interference experienced by each subcarrier in an MC-DS-CDMA system. The accuracy of (23) for a ZF equalizer in a BRAN A channel is demonstrated in Figure 6 by giving the average over channel realizations of the total interference power for a carrier frequency offset such that $N\Delta FT_s = 0.1$. For a Gaussian channel, it is easily proven that $I_{MC-DS-CDMA}[s' + k] = I_{MC-DS-CDMA}[s']$. This is due to the periodicity of function $\Psi_N(x)$ ($\Psi_N(x+1) = \Psi_N(x)$). In this case, the interference in MC-CDMA is equal to that in MC-DS-CDMA. The legend “mean MC-DS-CDMA” refers to the interference computed according to (23). For a MMSE equalizer and a time varying channel, the conclusions are different. The development of interference term for the pure MC-CDMA and MC-DS-CDMA systems in (21) yields

$$\begin{aligned}
 I_{MC-CDMA} &= \frac{\alpha \bar{P}}{N} \sum_{n'=0}^{N-1} \sum_{n=0}^{N-1} \left| \frac{L^* h[n] \psi_N(X^*) \psi_N(X^* + T^*)}{|H^* \psi_N(X^*)|^2 + \gamma} \right|^2 \\
 &\quad - \alpha \bar{P} \left| \frac{1}{N} \sum_{n'=0}^{N-1} \frac{|H^* \psi_N(X^*)|^2}{|H^* \psi_N(X^*)|^2 + \gamma} \right|^2 \\
 &\quad + \frac{\sigma^2}{N} \sum_{n'=0}^{N-1} \left| \frac{H^* \psi_N(X^*)}{|H^* \psi_N(X^*)|^2 + \gamma} \right|^2, \\
 I_{MC-DS-CDMA}[s'] &= \alpha \bar{P} \sum_{s=0}^{N-1} \left| \frac{H^{**} h[s] \psi_N(X^*) \psi_N(X^* + T^{**})}{|L^{**} \psi_N(X^*)|^2 + \gamma} \right|^2 \\
 &\quad - \alpha \bar{P} \left| \frac{|L^{**} \psi_N(X^*)|^2}{|L^{**} \psi_N(X^*)|^2 + \gamma} \right|^2 \\
 &\quad + \sigma^2 \left| \frac{L^{**} \psi_N(X^*)}{|L^{**} \psi_N(X^*)|^2 + \gamma} \right|^2,
 \end{aligned} \tag{24}$$

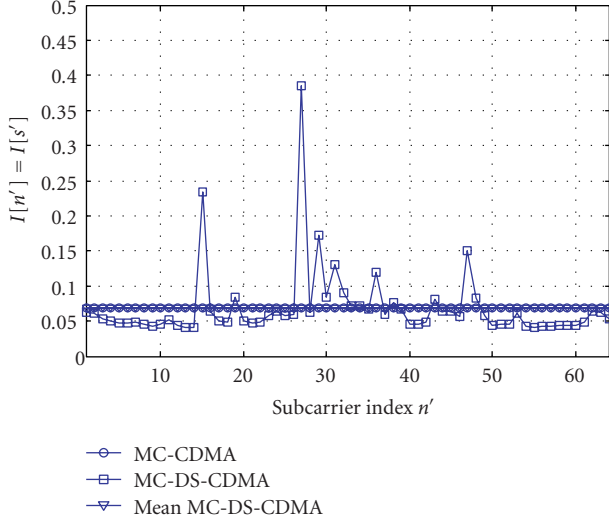


FIGURE 6: Mean interference power (ZF and BRAN A channel).

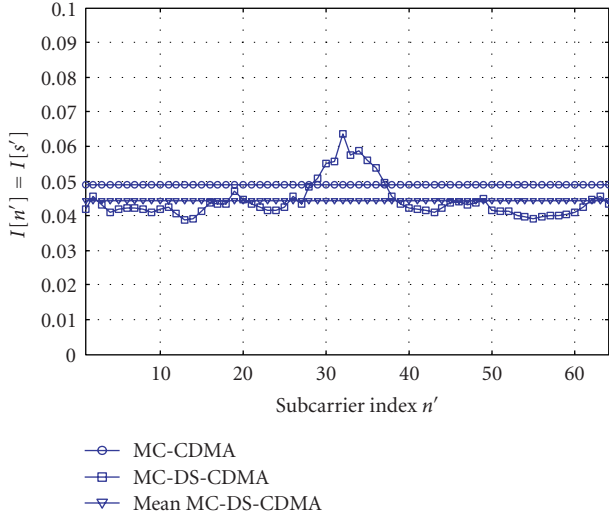


FIGURE 7: Mean interference power (MMSE and BRAN A channel).

where L^* denotes $h_{i',q'}^*[n']$, X^* denotes ΔFT_s , T^* denotes $(n' - n)/N$, H^* denotes $h_{i',q'}^*[n']$, H^{**} denotes $h_{i',q'}^*[s']$, T^{**} denotes $(s' - s)/N$ and L^{**} denotes $h_{i',q'}^*[s']$.

In (24), we are particularly interested by the second term of the interference components in each system. This term evaluates somewhat the self-interference power (It is proportional to the received useful power after equalization in each system.) Contrarily to the other terms in the interferences expressions, we can easily show that the mean value over subcarriers of the self-interference power in MC-DS-CDMA system is not equal to the power in MC-CDMA system. Moreover, the interpretation of this power is different in each system. In the case of MC-CDMA, it reflects the square of the mean of the self-interference magnitude. In MC-DS-CDMA, it reflects the mean of the square of the self-interference magnitude. These two magnitudes are equivalent only if the self-interference magnitude is the same in the two systems,

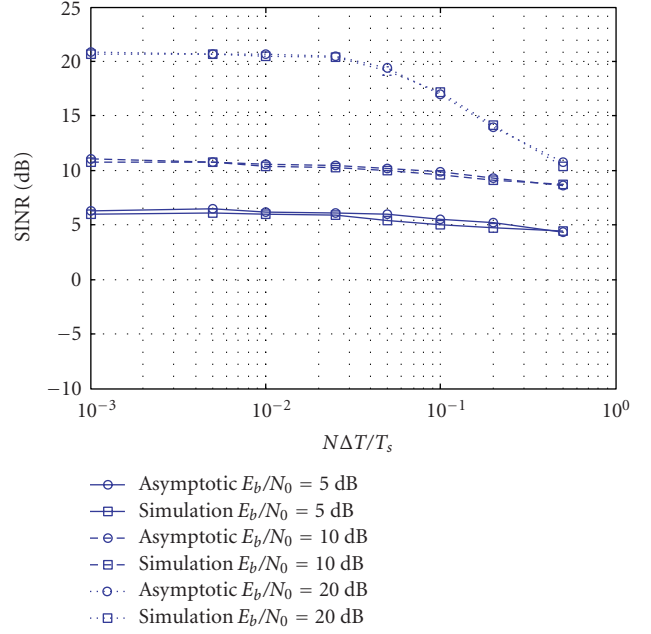


FIGURE 8: Validation of theoretical model (BRAN A channel).

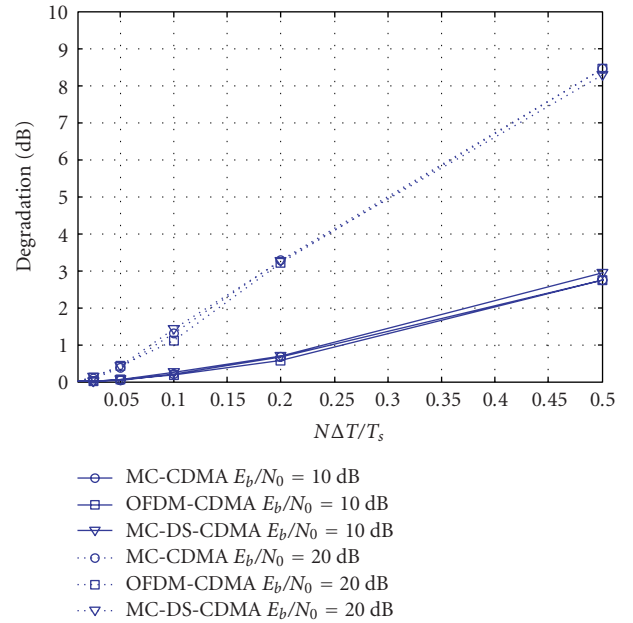


FIGURE 9: Comparison between degradation of different spreading schemes (Bran A channel, full load).

that is, when a ZF equalizer is used or if the channel is flat over the total bandwidth (Gaussian channel, e.g.). Moreover, the comparison allows us to conclude the interference in the pure MC-CDMA system is greater than that of the MC-DS-CDMA system. These results are very interesting since the comparison between the two systems is in reality a comparison between the MAI of MC-CDMA and the ICI of MC-DS-CDMA, respectively, using different types of equalizers. Unfortunately, the comparison between these

interferences is not obvious, since there is no equivalence between them. Figure 7 validates the previous comparisons and conclusions, where the MC-CDMA interference power is greater than the mean of interferences experienced in different subcarriers of MC-DS-CDMA.

4.2. Sampling frequency offset

When the sampling at the receiver is performed by means of a free running sampling whose frequency differs by a constant offset $1/\Delta T$ of the sampling at the transmitter, a normalized timing error linearly increases in time.

For a sampling frequency offset, (19) yields

$$\begin{aligned}
 E|I_0|^2 &= \frac{P_0}{N_F^2} \left| \sum_{n'=0}^{N_F-1} \frac{|h_{i',q'}[Y''] \psi_N((Y''/N)(\Delta T/T_s))|^2}{|h_{i',q'}[Y''] \psi_N((Y''/N)(\Delta T/T_s))|^2 + \gamma} \right|^2, \\
 I[s'] &= E|I_1|^2 + E|I_2|^2 + E|I_3|^2 + E|I_4|^2 \\
 &= \frac{\alpha \bar{P}}{N_F} \sum_{s=0}^{S-1} \sum_{n'=0}^{N_F-1} \sum_{n=0}^{N_F-1} \left| \frac{d_{i',q'}[s, n', n]}{y_{i',q'}[s, n', n]} \right|^2 \\
 &\quad - \frac{\alpha \bar{P}}{N_F} \left| \sum_{n'=0}^{N_F-1} \frac{|h_{i',q'}[Y''] \psi_N((Y''/N)(\Delta T/T_s))|^2}{|h_{i',q'}[Y''] \psi_N((Y''/N)(\Delta T/T_s))|^2 + \gamma} \right|^2 \\
 &\quad + \frac{\sigma^2}{N_F} \sum_{n'=0}^{N_F-1} \left| \frac{h_{i',q'}[Y''] \psi_N((Y''/N)(\Delta T/T_s))}{|h_{i',q'}[Y''] \psi_N((Y''/N)(\Delta T/T_s))|^2 + \gamma} \right|^2, \\
 E|I_3|^2 &= 0, \tag{25}
 \end{aligned}$$

where Y'' denotes $s'N_F + n'$, with

$$\begin{aligned}
 d_{i',q'}[s, n', n] &= h_{i',q'}^H[s'N_F + n'] h_q[sN_F + n] \\
 &\quad \cdot \psi_N \left(\frac{s'N_F + n' \Delta T}{N T_s} \right) \\
 &\quad \times \psi_N \left(\frac{sN_F + n \Delta T}{N T_s} + \frac{(s' - s)N_F + (n' - n)}{N} \right) \\
 y_{i',q'}[s, n', n] &= \left| h_{i',q'}[s'N_F + n'] \psi_N \left(\frac{s'N_F + n' \Delta T}{N T_s} \right) \right|^2 + \gamma. \tag{26}
 \end{aligned}$$

Figure 8 illustrates the comparison between theoretical and simulated mean SINRs of the fifth band ($s' = 5$) for an OFDM-CDMA system ($N_F \cdot N_T = 8 \times 4$), a BRAN A channel model, and a MMSE equalizer. It shows that our theoretical model matches perfectly with Monte Carlo simulations. Moreover, it shows that the sensitivity to sampling frequency offset becomes noticeable for $N\Delta T/T_s > 5\%$ depending on the E_b/N_0 level.

Figure 9 shows that MC-CDMA scheme ($N_F \cdot N_T = 32 \times 1$) is slightly less sensitive than OFDM-CDMA ($N_F \cdot N_T = 8 \times 4$) and MC-DS-CDMA ($N_F \cdot N_T = 1 \times 32$) systems to sampling frequency offset. Moreover, it shows that for a given signal bandwidth, this sensitivity increases with the number of carriers.

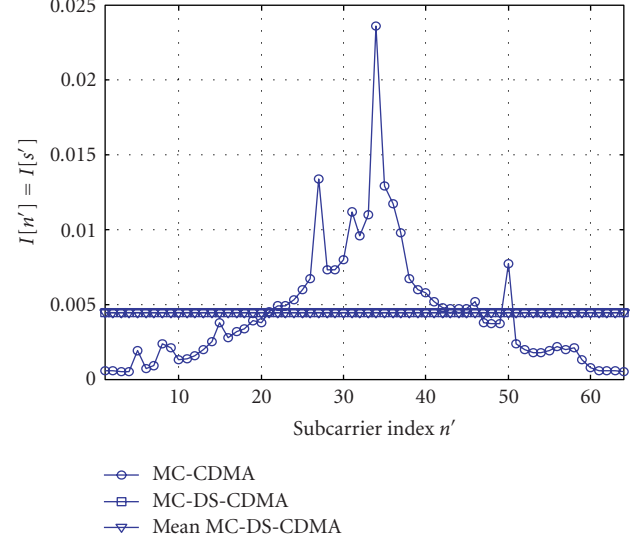


FIGURE 10: Mean interference power (ZF and BRAN A channel) $\Delta T/T_s = 390$ ppm.

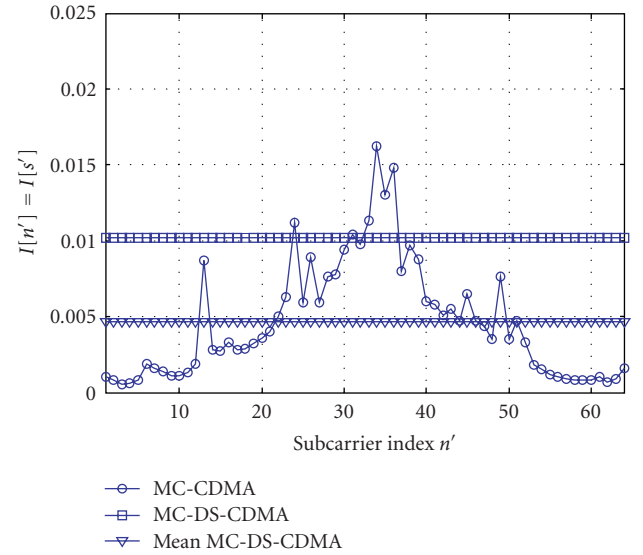


FIGURE 11: Mean interference power (MMSE and BRAN A channel) $\Delta T/T_s = 390$ ppm.

Again, we define $I_{MC-DS-CDMA}[s']$ the interference power of the (s')th subcarrier of a pure MC-DS-CDMA scheme and $I_{MC-CDMA}$ the total interference for a pure MC-CDMA system. We can easily show that (23) always holds, and similar conclusions for the interferences comparisons in the previous section can be given as shown with Figures 10 and 11.

4.3. Timing offset

In a timing offset situation, (19) becomes such complicated to expand for a frequency selective fading channel due to the complication of the side-to-side frequency equivalent

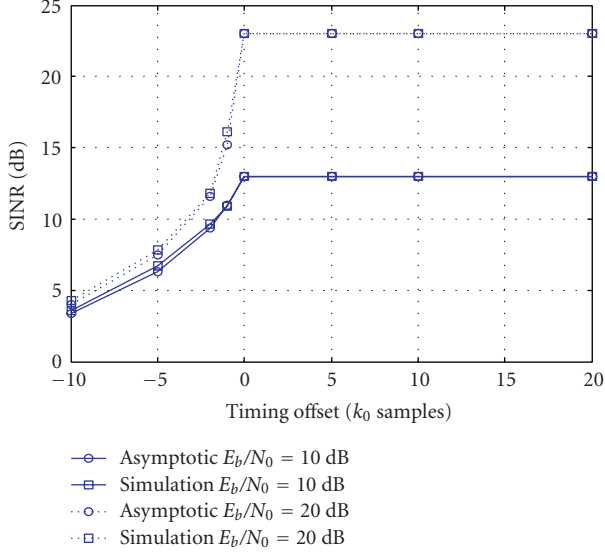


FIGURE 12: Validation of theoretical model (Gaussian channel).

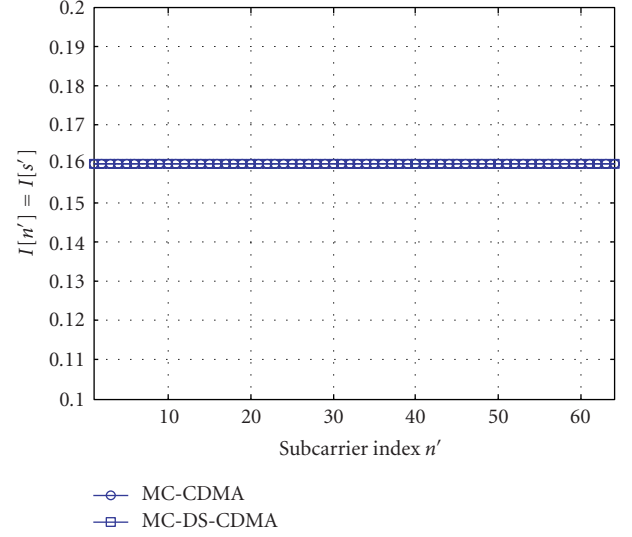
channel transfer function $\varphi_{r,i}(s', s, n', n, q', q)$. Thus, we restrict our analytical analysis to a Gaussian channel case, and we give simulation results for a selective fading channel. For a Gaussian channel, (19) yields the following: if $k_0 \geq 0$,

$$\begin{aligned} E|I_0|^2 &= P_0, \\ I[s'] &= \frac{\sigma^2}{1 + \gamma}, \end{aligned} \quad (27)$$

if $k_0 \leq 0$,

$$\begin{aligned} E|I_0|^2 &= P_0 \left| \frac{(N + k_0)^2}{(N + k_0)^2 + N^2 \gamma} \right|^2, \\ I[s'] &= \frac{\alpha \bar{P}}{N_F} \frac{(N + k_0)^2}{[(N + k_0)^2 + N^2 \gamma]^2} \\ &\quad \cdot \left\{ \sum_{s=0}^{S-1} \sum_{n'=0}^{N_F-1} \sum_{n=0}^{N_F-1} \right. \\ &\quad \times \left[\left| \frac{\sin(\pi(((s' - s)N_F + n' - n)/N)(N + k_0))}{\sin(\pi(((s' - s)N_F + n' - n)/N))} \right|^2 \right. \\ &\quad \left. \left. + 2 \left| \frac{\sin(\pi(((s' - s)N_F + n' - n)/N)k_0)}{\sin(\pi(((s' - s)N_F + n' - n)/N))} \right|^2 \right] \right\} \\ &\quad - \alpha \bar{P} \frac{(N + k_0)^4}{[(N + k_0)^2 + N^2 \gamma]^2} + \sigma^2 \frac{(N + k_0)^2 N^2}{[(N + k_0)^2 + N^2 \gamma]^2}. \end{aligned} \quad (28)$$

Due to the periodicity of the function $f_N(n') = \sum_{n=0}^{N-1} |\sin(\pi((n' - n)/N)\chi) / \sin(\pi((n' - n)/N))|^2$ with respect to the variable χ , we can easily show from (28) that the interference of a pure MC-CDMA system is equal to the interference of a pure MC-DS-CDMA for a Gaussian

FIGURE 13: Interference power (MMSE and Gaussian channel) $k_0 = -5$ samples.

channel. This means that (23) always holds. To derive simulation results, we first compare the asymptotical SINR deduced from (17) and (28) with SINR obtained by Monte Carlo simulations as shown in Figure 12. This figure shows that when the receiver FFT window is in delay with respect to the transmitter one (i.e., $k_0 < 0$), the degradation of the SINR increases rapidly. An FFT window error equal to 2 samples degrades the SINR of 2 dB for a $E_b/N_0 = 10$ dB. Greater degradation is observed for higher E_b/N_0 . Similar results are already presented in our previous work in [13] for a Bran A channel model.

Figure 13 shows the accuracy of the conclusion predicted by (23) and (28) for a Gaussian channel and full load system. This conclusion does not hold for a frequency selective fading channel and a MMSE equalizer as shown in Figure 14.

Figure 15 shows that the three spreading schemes (MC-CDMA, OFDM-CDMA, and MC-DS-CDMA) are similarly sensitive to timing offset. Notice that in this figure the degradation is zero for a timing offset k_0 such that $0 \leq k_0 \leq (v - W \cong 15)$, since this interval of k_0 corresponds to a good timing window at the receiving side, that is, the receiver is perfectly synchronized with the transmitter.

5. CONCLUSION

In this article, we have investigated the effect of three synchronization errors on the performance of two-dimensional OFDM-CDMA spreading schemes. A new analytical expression of the SINR has been derived. It is valid for various kinds of single user equalizer (MMSE, ZF) and for any frequency selective channel. It is independent of the actual value of the spreading codes but takes their orthogonality into account. Exploiting this model, we found that for a ZF equalizer, the total interference power of a MC-CDMA system is the average of the interference experienced by each subcarrier in a MC-DS-CDMA system. Moreover, we have shown that the

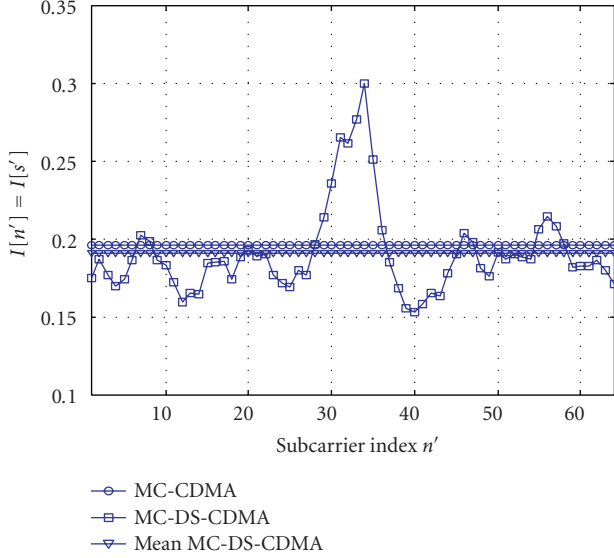


FIGURE 14: Interference power (MMSE and Bran A channel) $k_0 = -5$ samples.

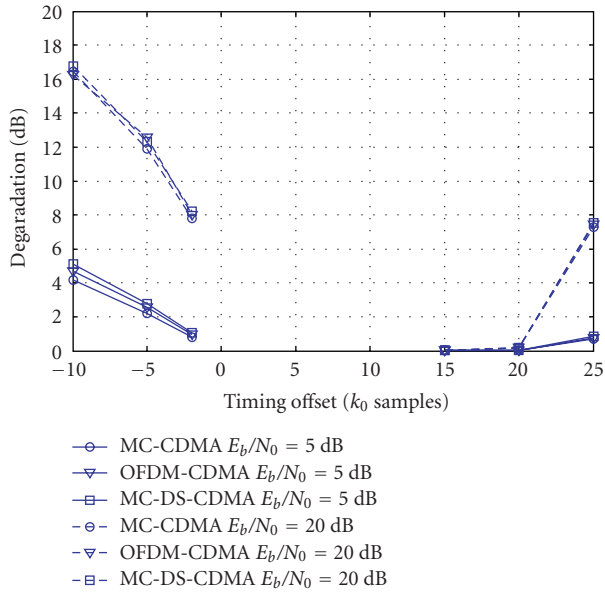


FIGURE 15: Comparison between degradation of different spreading schemes (Bran A channel, full load).

three spreading schemes (MC-CDMA, OFDM-CDMA, and MC-DS-CDMA) are similarly sensitive to synchronization error whatever the load is.

APPENDICES

A. EQUIVALENT DISCRETE CHANNEL TRANSFER FUNCTION

In this section, we derive the analytical expression of the equivalent discrete-time discrete-frequency channel transfer

function deduced from a continuous model which includes the pulse shaping transmitter filter $v(t)$, the base band continuous-time multipath channel $g_q(t)$, and the pulse shaping receiver filter $v^*(-t)$ ($*$ stands for complex conjugate). The model takes into account the occurrence of any synchronization error at the receiving side and can be used for the OFDM case as well as for OFDM-CDMA case.

Without loss of generality, we assume first that we transmit sequences of $(N + \nu)$ samples which may correspond to OFDM symbols and the receiver generates a constant timing offset of k_0 samples, a carrier frequency offset ΔF , and a sampling frequency offset $1/\Delta T$. We assume also that the sampling and carrier errors linearly increase during a sequence of $(N + \nu)$ samples only, that is, they are set to zero at the beginning of each sequence. The equivalent channel transfer function can then be modeled by Figure 16.

At the receiving side, the signal can be written as the convolution of the transmitted signal with the transmitting pulse shaping filter, the multipath channel response $g_q(t)$, and the receiver pulse shaping filter. Assuming that the relative carrier frequency offset is slowly variant as compared to the duration of the receiving pulse shaping filter ($\Delta F \cdot T_s \ll 1$), the received (u)th sample of the (q')th sequence can be written as

$$r_{q'}[u] = \sum_{q=q'-1}^{q'+1} \sum_{k=-\nu}^{N-1} x_q[k] \int_{p=-\infty}^{\infty} \gamma_v(p) g_q \{ \hat{t}_{q',u} - t_{q,k} - p \} \times \exp \{ j2\pi u \Delta F T_s \} dp, \quad (\text{A.1})$$

where $x_q[k]$ is the k th transmitted sample of the q th sequence, transmitted at instant $t_{q,k} = [q(N + \nu) + k]T_s$, $\gamma_v = v^* v^H$ is the analog convolution between transmit and receive pulse shaping filters, and $\hat{t}_{q',u} = t_{q',u} + k_0 T_s + u \Delta T$ represents the sampling time at the receiver. Therefore, the received signal can be written in an equivalent form as

$$r_{q'}[u] = \sum_{q=q'-1}^{q'+1} \sum_{k=-\nu}^{N-1} g_{q',q}^{\text{eq}}[u - k; u] x_q[k]. \quad (\text{A.2})$$

In this more compact model, $g_{q',q}^{\text{eq}}[k; u]$ is the equivalent discrete channel impulse response deduced from the equivalent continuous-time channel impulse response $g_{q',q}^{\text{eq}}(\tau; u)$ by $g_{q',q}^{\text{eq}}[k; u] = g_{q',q}^{\text{eq}}(\tau; u)|_{\tau=kT_s}$, where

$$g_{q',q}^{\text{eq}}(\tau; u) = \int_{p=-\infty}^{\infty} \gamma_v(p) g_q((q' - q)(N + \nu) + \tau + k_0 T_s + u \Delta T - p) \cdot \exp(j2\pi u \Delta F T_s) dp. \quad (\text{A.3})$$

Moreover, the double indexes (q', q) indicate that the channel is applied on the q th sequence, however, its effect is measured on the (q') th sequence. It traduces the effect of the ISI.

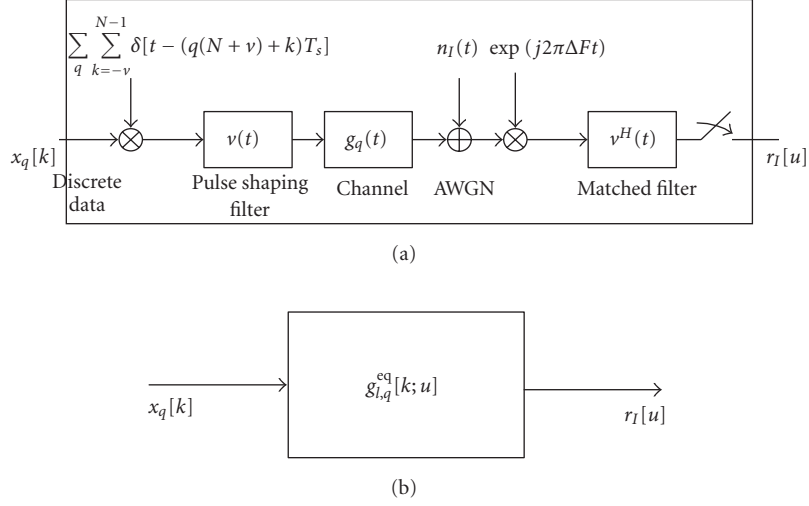


FIGURE 16: Equivalent channel transfer function with synchronization errors.

The equivalent (continuous frequency) channel transfer function can be written as the Fourier transform (FT) of (A.3) with respect to the variable τ . It is given by

$$\begin{aligned}
 h_{q',q}^{eq}(f; u) &= |V(f)|^2 \exp(j2\pi\beta f T_s) \\
 &\times \exp\left[j2\pi f(u\Delta T + k_0 T_s)\right] \\
 &\cdot \exp(j2\pi f u \Delta F T_s) \sum_{k=M_1}^{M_2} g_q(k) \exp(-j2\pi f k) \\
 &\text{with } M_1 = [u - (N-1)T_s + \beta T_s + u\Delta T + k_0 T_s], \\
 M_2 &= (u + v)T_s + \beta T_s + u\Delta T + k_0 T_s, \\
 \beta &= (q' - q)(N + v).
 \end{aligned} \tag{A.4}$$

Assuming that $|V(f)|^2 = 1$ for $f \in [-1/(2T_s), 1/(2T_s)]$ and zero elsewhere, the discrete-time discrete-frequency channel transfer function can be deduced from (A.4) for $f = n/(NT_s)$ by

$$\begin{aligned}
 h_{q',q}^{eq}[n; u] &= \exp\left(j2\pi\beta \frac{n}{N} T_s\right) \exp\left[j2\pi \frac{n}{N} (u\Delta T + k_0 T_s)\right] \\
 &\cdot \exp\left(j2\pi \frac{n}{N} u \Delta F T_s\right) \times \sum_{l=M_1}^{M_2} g_q[l] \exp\left(-j2\pi \frac{n}{N} l\right).
 \end{aligned} \tag{A.5}$$

In (A.5), the sum over k represents the FFT of a part of the channel impulse response depending on the timing error k_0 . Thus, for a perfect synchronized system, $h_{q',q}^{eq}[n; u]$ becomes independent of the time variable u , and the symbol index q : it represents $h_{q'}[n]$, the FFT on the subcarrier n of the discrete equivalent low-pass channel $g_{q'}[k]$. When there is no timing error ($k_0 = 0$), (A.5) yields

$$h_{q',q}^{eq}[n; u] = h_{q'}[n] \exp\left[j2\pi \frac{n}{N} (u\Delta T)\right] \exp(j2\pi u \Delta F T_s). \tag{A.6}$$

Eventually, in the case of OFDM-CDMA transmission, each OFDM symbol can be identified by the index q' (resp., q) of the (i')th (resp., i)th OFDM-CDMA symbol. Therefore, (A.5) and (A.6) can be written as

$$\begin{aligned}
 h_{i'N_T+q',iN_T+q}^{eq}[n; u] &= \exp\left(j2\pi\beta \frac{n}{N} T_s\right) \\
 &\times \exp\left[j2\pi \frac{n}{N} (u\Delta T + k_0 T_s)\right] \\
 &\times \exp\left(j2\pi \frac{n}{N} u \Delta F T_s\right) \\
 &\times \sum_{l=M_1}^{M_2} g_q[l] \exp\left(-j2\pi \frac{n}{N} l\right) \\
 &\text{with } \beta = [(i' - i)N_T + q' - q](N + v),
 \end{aligned} \tag{A.7}$$

$$\begin{aligned}
 h_{i'N_T+q',iN_T+q}^{eq}[n; u] &= h_{i'N_T+q'}[n] \exp\left[j2\pi \frac{n}{N} (u\Delta T)\right] \\
 &\times \exp\left(j2\pi \frac{n}{N} u \Delta F T_s\right).
 \end{aligned} \tag{A.8}$$

B. ASYMPTOTIC RESULTS

In this section, the three properties from the RM and FP theories are first defined. Then, their application for the computation of (19) is detailed.

Property 1. First, we use a property initially applied in [18]. It assumes that each sequence is itself random. This assumption can be justified by the use of random scrambling codes conjointly with spreading sequences. Thus,

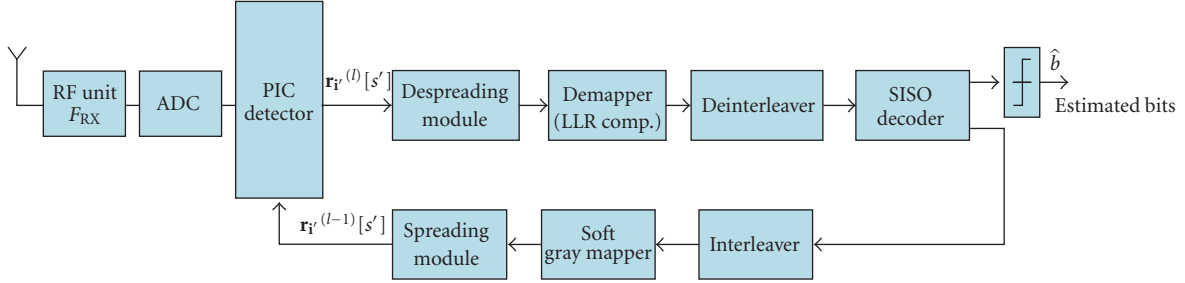


FIGURE 17: Iterative receiver scheme.

if \mathbf{A} is a $N_c \cdot N_c$ uniformly bounded deterministic matrix and $\mathbf{c}_m = (1/\sqrt{N_c})(c_m(0), \dots, c_m(N_c - 1))^T$, where $c_m(l)$'s are i.i.d. complex random variables with zero mean, unit variance, and finite eighth-order moment, then [18] yields

$$\mathbf{c}_m^H \mathbf{A} \mathbf{c}_m \xrightarrow{N_c \rightarrow \infty} \frac{1}{N_c} \text{tr}(\mathbf{A}), \quad (\text{B.1})$$

where \mathbf{c}_0 is obtained by the multiplication of a WH sequence with a long scrambling code. Hence, the assumptions needed for (B.1) are easily satisfied. This property is used to evaluate $E|I_0|^2$, $E|I_1|^2$, $E|I_2|^2$, and $E|I_3|^2$.

Property 2. Let \mathbf{C} a Haar distributed unitary matrix of size $N_c \cdot N_u$ [11]. \mathbf{C} can be decomposed into a vector \mathbf{c}_0 of size N_c and a matrix \mathbf{U} of size $N_c \cdot (N_u - 1)$. So, \mathbf{C} can be written as $\mathbf{C} = (\mathbf{c}_0, \mathbf{U})$. Given these hypotheses, it is proven in [12] that

$$E[\mathbf{U} \mathbf{Q} \mathbf{U}^H | \mathbf{c}_0] = \alpha \bar{P} (\mathbf{I} - \mathbf{c}_0 \mathbf{c}_0^H), \quad \text{when } N_c \rightarrow \infty, \quad (\text{B.2})$$

where $\alpha = N_u/N_c$ is the system load, and $\bar{P} = (1/(N_u - 1)) \sum_{m=1}^{N_u-1} P_m$ is the average power of the interfering users. The Haar distributed assumption is only technical and will not change in the total result. The simulation results obtained in [11] with a WH spreading matrix match well with the theoretical model. This lemma is used to evaluate $E|I_1|^2$.

Property 3. If \mathbf{C} is generated from a $N_c \cdot N_c$ Haar unitary RM, then matrices $\mathbf{C}[s] \mathbf{Q} \mathbf{C}^H[s]$ and $\mathbf{Z}[s']^H \mathbf{H}[s', s] \mathbf{H}[s', s] \mathbf{Z}[s']$ are asymptotically free almost everywhere [21]. In other words, verifying the above conditions, one can conclude that

$$\begin{aligned} & \frac{1}{N_c} \text{tr}(\mathbf{Z}[s']^H \mathbf{H}[s', s] \mathbf{C}[s] \mathbf{P} \mathbf{C}^H[s] \mathbf{H}[s', s] \mathbf{Z}[s']^H) \\ & \xrightarrow{N_c \rightarrow \infty} \frac{1}{N_c} \text{tr}(\mathbf{Z}[s']^H \mathbf{H}[s', s] \mathbf{H}[s', s] \mathbf{H}[s', s] \mathbf{Z}[s']^H) \\ & \cdot \frac{1}{N_c} \text{tr}(\mathbf{C}[s] \mathbf{P} \mathbf{C}^H[s]). \end{aligned} \quad (\text{B.3})$$

For definition of freeness, the reader may refer to [11] for more details.

Assuming that $\mathbf{c}_0[s']$ is random, (B.1) is used to evaluate $E|I_0|^2$. Since we use a long scrambling code, $\mathbf{c}_0[s']$ and $\mathbf{C}[s]$ are independent for $s' \neq s$. Using (B.1), $E|I_2|^2$ becomes

$$E|I_2|^2 = \sum_{\substack{s=0 \\ s \neq s'}}^{S-1} \text{tr}(\mathbf{Z}[s']^H \mathbf{H}[s', s] \mathbf{C}[s] \mathbf{P} \mathbf{C}^H[s] \mathbf{H}[s', s] \mathbf{Z}[s']^H). \quad (\text{B.4})$$

This computation method has initially been applied for the analysis of multicell downlink CDMA systems in [22]. Applying (B.2) for the computations of $E|I_1|^2$ and (B.3) for the computations of $E|I_2|^2$ in (B.4) as well as for the computation of $E|I_3|^2$, (19) is obtained.

C. ITERATIVE EQUALIZER

In this section, we give a brief overview about a sophisticated iterative equalizer used to reduce the interference due to the synchronisation errors. The iterative detector shown in Figure 17 is made of a parallel interference canceller (PIC), a despreader, a log likelihood ratio (LLR) computation module [23], a soft-input soft-output (SISO) decoder [24] (a convolutional encoder is used at the transmitter), a soft mapper, and a spreader. The spreading and despreading modules contain implicitly the 2D chip mapping and demapping modules, respectively. The solution proposed here consists of an iterative process, where the PIC detector and channel decoder exchange extrinsic information in an iterative way until the algorithm converges. The iterative detection and decoding exploit the error correction capabilities of the channel code to provide improved performance. This is achieved by iteratively passing soft a priori information between the detector and the soft-input soft-output (SISO) decoder [24]. However, such a receiver needs the knowledge of the spreading codes in order to generate the transmitted symbols.

At the first iteration ($l = 1$), after equalization and despreading, the demapper takes the symbols estimated (according to (15)) for all users $\hat{a}_{i', m}[s']$, the knowledge of the channel $\mathbf{H}_{i', i'}[s', s']$ and the noise variance, and computes the LLR values (soft information) of each of the coded bits transmitted per channel use. The deinterleaved soft information at the output of the demapper becomes the input of the outer decoder. The outer SISO decoder computes the a posteriori information of the information bits and of the coded bits. The a posteriori information of the coded bits produces new (and hence) extrinsic LLR information of the coded bits upon removal of the a priori information (When the transmitted bits are likely equal, this information is equal to zero.) and minimizing the correlation between input values. In our work, SISO decoding is based on the Max-Log-MAP algorithm [24]. The extrinsic information at the output of the channel decoder is then interleaved and fed to the soft Gray mapper module. The soft mapper achieves reciprocal

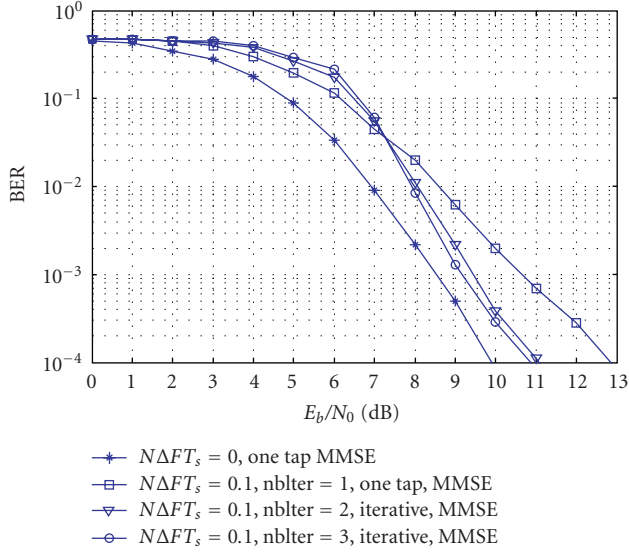


FIGURE 18: BER performance of iterative receiver in OFDM-CDMA system, Bran A channel, and 16-QAM constellation.

operation of the demapper. It leads to a first estimation of the transmitted symbols in the different subbands.

Knowing the different spreading codes, we are now able to generate approximately the different interferences terms of (15) and to cancel them from the useful signal. The approximation in the interference generation is due to the fact that we are able to estimate only the channel matrix $\mathbf{H}_{i',i}[s',s]$, that is, we cannot generate the matrix $\mathbf{H}_{i',i}[s',s]$ (where $i' \neq i$ and $s' \neq s$).

Let $\mathbf{r}_i^{(l)}[s'] = [R_{i',0}[s'N_F], \dots, R_{i',N_F-1}[s'N_F + N_F - 1]]^T$ be the column vector composed of the frequency received signals $R_{i',q'}[s'N_F + n']$ ($q' = 1, \dots, N_T; n' = 0, \dots, N_F$) at the output of the FFT (see (8)) of the iteration l . At the succeeding iterations ($l > 1$), the equalization matrix $\mathbf{Z}_i[s']$ is applied on the following vector:

$$\begin{aligned} \tilde{\mathbf{r}}_i^{(l)}[s'] &= \mathbf{r}_i^{(l-1)}[s'] - \mathbf{H}_{i',i}[s',s']\mathbf{U}[s']\mathbf{Q}[s]\tilde{\mathbf{a}}_i^{(l-1)}[s'] \\ &\quad - \sum_{\substack{s=0 \\ s \neq s'}}^{S-1} \mathbf{H}_{i',i'}[s',s']\mathbf{C}[s]\mathbf{P}[s]\mathbf{a}_i^{(l-1)}[s]. \end{aligned} \quad (\text{C.1})$$

In (C.1), we do not consider the ISI for simplicity reasons.

Once they are equalized, the different signals of (C.1) are fed to the despreading and demapping modules, and then to the SISO decoder. The PIC detector and the SISO decoder exchange information until the algorithm converges.

In order to characterize the behavior of the iterative equalizer, we give the results in the presence of the CFO in terms of bit error rate (BER) instead of the SINR. Figure 18 gives the BER performance versus the E_b/N_0 ratio for different number of iterations in the OFDM-CDMA system with a 16-QAM constellation, a coding rate $R = 1/2$ using a convolutional encoder, and a Bran A channel model. We show in this figure the convergence of the iterative equalizer after 3 iterations. Also, a gain of approximately 2 dB

in terms of E_b/N_0 is obtained after 3 iterations. However, this will be to the detriment of a complexity increase.

ACKNOWLEDGMENT

The authors would like to thank the reviewers for their precious comments, reviews, and remarks. Parts of this work have been presented in [13, 14, 25].

REFERENCES

- [1] N. Maeda, Y. Kishiyama, H. Atarashi, and M. Sawahashi, "Variable spreading factor-OFCDM with two dimensional spreading that prioritizes time domain spreading for forward link broadband wireless access," in *Proceedings of the 57th IEEE Semiannual Vehicular Technology Conference (VTC '03)*, vol. 1, pp. 127–132, Jeju, Korea, April 2003.
- [2] A. Persson, T. Ottosson, and E. Ström, "Time-frequency localized CDMA for downlink multi-carrier systems," in *Proceedings of the 7th IEEE International Symposium on Spread Spectrum Techniques and Applications*, vol. 1, pp. 118–122, Prague, Czech Republic, September 2002.
- [3] T. Pollet, M. Van Bladel, and M. Moeneclaey, "BER sensitivity of OFDM systems to carrier frequency offset and Wiener phase noise," *IEEE Transactions on Communications*, vol. 43, no. 2–4, part 1, pp. 191–193, 1995.
- [4] P. H. Moose, "A technique for orthogonal frequency division multiplexing frequency offset correction," *IEEE Transactions on Communications*, vol. 42, no. 10, pp. 2908–2914, 1994.
- [5] H. Steendam and M. Moeneclaey, "Optimisation of OFDM on frequency-selective time selective fading channels," in *Proceedings of the URSI International Symposium on Systems, Signals and Electronics (ISSSE '98)*, pp. 398–403, Pisa, Italy, September–October 1998.
- [6] H. Steendam and M. Moeneclaey, "The effect of synchronization errors on MC-CDMA performance," in *Proceedings of the IEEE International Conference on Communications (ICC '99)*, pp. 1510–1514, Vancouver, Canada, June 1999.
- [7] H. Steendam and M. Moeneclaey, "Comparison of the sensitivities of MC-CDMA and MC-DS-CDMA to carrier frequency offset," in *Proceedings of Symposium on Communications and Vehicular Technology (SCVT '00)*, pp. 166–173, Leuven, Belgium, October 2000.
- [8] H. Steendam and M. Moeneclaey, "The effect of clock frequency offsets on downlink MC-DS-CDMA," in *Proceedings of the 7th IEEE International Symposium on Spread Spectrum Techniques and Applications*, vol. 1, pp. 113–117, Prague, Czech Republic, September 2002.
- [9] Y. Z. Luan, J. W. Yang, Y. C. Sun, and J. D. Li, "Performance analysis of the multi-user receiver exploited in MC-CDMA system," in *Proceedings of the 2nd International Conference on 3G Mobile Communication Technologies*, pp. 378–382, London, UK, March 2001.
- [10] G. A. Al-Rawi, T. Y. Al-Naffouri, A. Bahai, and J. Cioffi, "An iterative receiver for coded OFDM systems over time-varying wireless channels," in *Proceedings of the IEEE International Conference on Communications (ICC '03)*, vol. 5, pp. 3371–3376, Anchorage, Alaska, USA, May 2003.
- [11] M. Debbah, W. Hachem, P. Loubaton, and M. de Courville, "MMSE analysis of certain large isometric random precoded systems," *IEEE Transactions on Information Theory*, vol. 49, no. 5, pp. 1293–1311, 2003.

- [12] J.-M. Chaufray, W. Hachem, and P. Loubaton, "Asymptotical analysis of optimum and sub-optimum CDMA downlink MMSE receivers," *IEEE Transactions on Information Theory*, vol. 50, no. 11, pp. 2620–2638, 2004.
- [13] Y. Nasser, M. des Noes, L. Ros, and G. Jourdain, "SINR estimation of OFDM-CDMA systems with constant timing offset: a large system analysis," in *Proceedings of the 16th IEEE International Symposium on Personal, Indoor and Mobile Radio Communications (PIMRC '05)*, vol. 1, pp. 432–436, Berlin, Germany, September 2005.
- [14] Y. Nasser, M. des Noes, L. Ros, and G. Jourdain, "The effect of clock frequency offset on OFDM-CDMA systems performance," in *Proceedings of the 12th IEEE Symposium on Communications and Vehicular Technology (SCVT '05)*, Enschede, The Netherlands, November 2005.
- [15] N. Yee, J. P. Linnartz, and G. Fettweis, "Multi-carrier CDMA for indoor wireless radio networks," in *Proceedings of the 4th IEEE International Symposium on Personal Indoor and Mobile Radio Communications (PIMRC '93)*, pp. 109–113, Yokohama, Japan, September 1993.
- [16] V. M. da Silva and E. S. Sousa, "Performance of orthogonal CDMA sequences for quasi-synchronous communication systems," in *Proceedings of the 2nd International Conference on Universal Personal Communications (ICUPC '93)*, pp. 995–999, Ottawa, Canada, October 1993.
- [17] D. N. C. Tse and S. V. Hanly, "Linear multiuser receivers: effective interference, effective bandwidth and user capacity," *IEEE Transactions on Information Theory*, vol. 45, no. 2, pp. 641–657, 1999.
- [18] J. Evans and D. N. C. Tse, "Large system performance of linear multiuser receivers in multipath fading channels," *IEEE Transactions on Information Theory*, vol. 46, no. 6, pp. 2059–2078, 2000.
- [19] P. Jallon, M. des Noes, D. Ktenas, and J.-M. Brossier, "Asymptotic analysis of the multiuser MMSE receiver for the downlink of a MC-CDMA system," in *Proceedings of the 57th IEEE Semiannual Vehicular Technology Conference (VTC '03)*, vol. 1, pp. 363–367, Jeju, Korea, April 2003.
- [20] J. Medbo, H. Andersson, P. Schramm, and H. Asplund, "Channel models for HIPERLAN/2 in different indoor scenarios," Tech. Rep. COST 259, TD98, University of Bradford, Bradford, UK, April 1998.
- [21] W. Hachem, "Simple polynomial detectors for CDMA downlink transmissions on frequency-selective channels," *IEEE Transactions on Information Theory*, vol. 50, no. 1, pp. 164–171, 2004.
- [22] T. B. Abdallah and M. Debbah, "Downlink CDMA: to cell or not to cell," in *Proceedings of the 12th European Signal Processing Conference (EUSIPCO '04)*, Vienna, Austria, September 2004.
- [23] F. Tosato and P. Bisaglia, "Simplified soft-output demapper for binary interleaved COFDM with application to HIPERLAN/2," in *Proceedings of the IEEE International Conference on Communications (ICC '02)*, vol. 2, pp. 664–668, New York, NY, USA, April-May 2002.
- [24] J. Hagenauer and P. Hoeher, "A viterbi algorithm with soft-decision outputs and its applications," in *Proceedings of the IEEE Global Telecommunications Conference and Exhibition (GLOBECOM '89)*, vol. 3, pp. 1680–1686, Dallas, Tex, USA, November 1989.
- [25] Y. Nasser, M. des Noes, L. Ros, and G. Jourdain, "Sensitivity of OFDM-CDMA systems to carrier frequency offset," in *Proceedings of the IEEE International Conference on Communications (ICC '06)*, vol. 10, pp. 4577–4582, Istanbul, Turkey, June 2006.